Laser Physics

Astro Ltd.

PAPER • **OPEN ACCESS**

Laser photoacoustic technique for ultrasonic surface acoustic wave velocity evaluation on porcelain

To cite this article: K Qian *et al* 2016 *Laser Phys.* **26** 106101

View the article online for updates and enhancements.

Related content

- Effect of a pulsed Nd:YAG laser on surface acoustic wave velocity of human dental enamel
S J Tu, L Zhan, K Qian et al.
- Laser Ultrasonic Technique for Evaluating Human Dental Enamel
D H-C Wang, S Fleming, Y-C Lee et al.
- Non-contact thickness gauging of a thin film using surface waves and a void effect on their propagation
S Fourez, F Jenot, M Ouaftouh et al.

Recent citations

- Introducing the *Laser Physics* and *Laser Physics Letters* highlights of 2016
Jarlath McKenna
- Introducing the *Laser Physics* and *Laser Physics Letters* highlights of 2016
Jarlath McKenna

This content was downloaded from IP address 117.211.180.23 on 17/01/2018 at 09:21

OPEN ACCESS
IOP Publishing | Astro Ltd
Laser Physics
Laser Phys. **26** (2016) 106101 (4pp)
doi:10.1088/1054-660X/26/10/106101

Laser photoacoustic technique for ultrasonic surface acoustic wave velocity evaluation on porcelain

K Qian[1], S J Tu[2], L Gao[1], J Xu[1], S D Li[1], W C Yu[1] and H H Liao[1]

[1] School of Information Engineering, Hubei University for Nationalities, Enshi 445000, Hubei Province, People's Republic of China
[2] Eoptolink Technology Inc. Ltd., No.127 West Wulian Street, Chengdu 610213, Sichuan Province, People's Republic of China

E-mail: Kaiqian@sjtu.org

Received 29 July 2016
Accepted for publication 7 August 2016
Published 6 September 2016

Abstract

A laser photoacoustic technique has been developed to evaluate the surface acoustic wave (SAW) velocity of porcelain. A Q-switched Nd:YAG laser at 1064 nm was focused by a cylindrical lens to initiate broadband SAW impulses, which were detected by an optical fiber interferometer with high spatial resolution. Multiple near-field surface acoustic waves were observed on the sample surface at various locations along the axis perpendicular to the laser line source as the detector moved away from the source in the same increments. The frequency spectrum and dispersion curves were obtained by operating on the recorded waveforms with cross-correlation and FFT. The SAW phase velocities of the porcelain of the same source are similar while they are different from those of different sources. The marked differences of Rayleigh phase velocities in our experiment suggest that this technique has the potential for porcelain identification.

Keywords: laser ultrasonics, porcelains, surface acoustic wave

(Some figures may appear in colour only in the online journal)

1. Introduction

The study of surface characteristics, such as density, Young's modulus and the roughness of ceramics, is one of the most significant tasks in archaeology. The surface characteristics are different from one to another due to their provenance, age and manufacturing process. Since the 18th century, archaeologists, historians, chemists and physicists have developed a variety of methods to study artifacts and ancient objects [1, 2]. Among the various techniques, elemental analysis is the most widely used method, but most of them are destructive or require sample preparation. Relying largely on the progress in modern techniques and data analysis systems, the study on ceramics has been developed rapidly in the last 50 years.

Presently, the most prevalent methods used for the characterization of a broad variety of ancient artifacts are: neutron activation analysis [3, 4], inductively coupled plasma atomic emission spectroscopy [5, 6], inductively coupled plasma mass spectrometry (ICP-MS) [7, 8], x-ray fluorescence (XRF) [9, 10], and laser induced breakdown spectroscopy [11]. ICP-MS analysis has high detection accuracy and it is ideal for element analysis. However, the procedure takes a relatively long time. XRF has been quite attractive in elemental analysis, particularly with the development of portable instruments. However, the XRF has a very low lateral spatial resolution. Among the most popular methods, there is little or no one using photoacoustic techniques. Due to their flexibility, simplicity and maneuverability, photoacoustic techniques have been widely used in nondestructive evaluation [12–14].

Original content from this work may be used under the terms of the Creative Commons Attribution 3.0 licence. Any further distribution of this work must maintain attribution to the author(s) and the title of the work, journal citation and DOI.

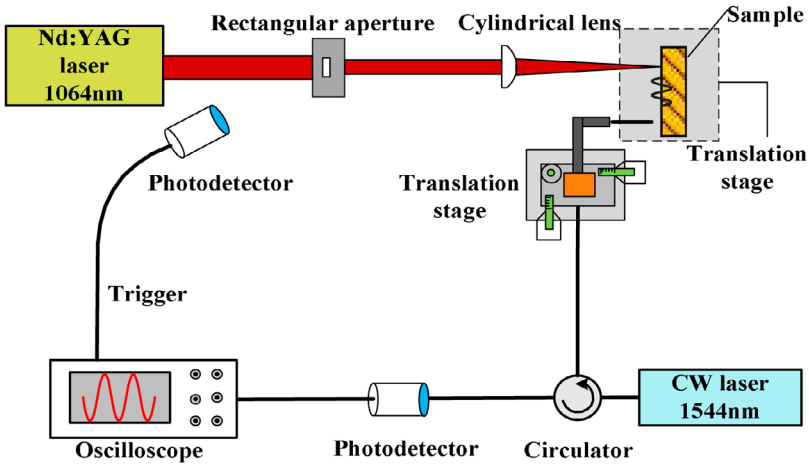

Figure 1. Experimental configuration for the generation and detection of Rayleigh waves.

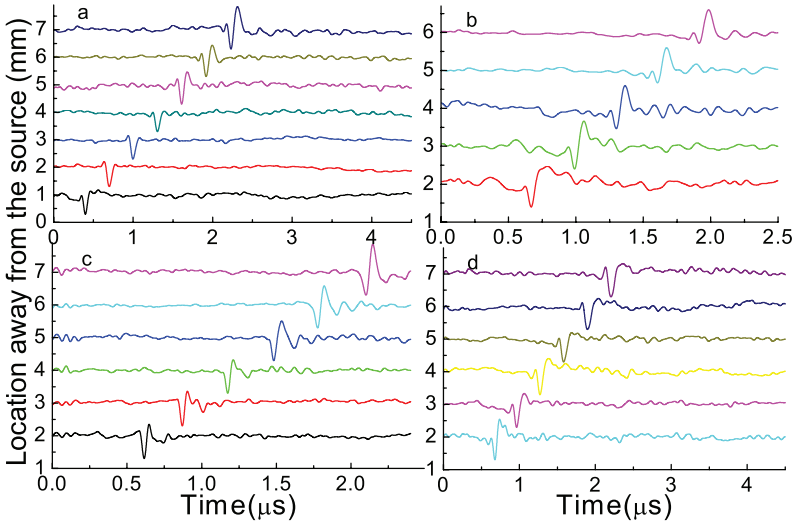

Figure 2. Typical Rayleigh waves detected at various locations on different samples (a) A1, (b) A2, (c) B, (d) C1.

In our experiment, it is the first time that we utilize the laser photoacoustic methods for Rayleigh wave velocity evaluation on porcelain. The optical fiber interferometer was first proposed by Wang *et al* [15]. Since using a pulse laser and simple optical fiber interferometer for generating and detecting acoustic waves respectively, the experiment procedure becomes flexible and straightforward.

2. Principle and experiments

A surface acoustic wave, also known as the Rayleigh wave, is a type of elastic ultrasound. During the process of propagation, its amplitude decays with depth exponentially. The velocity of the Rayleigh wave depends on the elastic parameters and the density of the material. In an homogeneous isotropic medium, the velocity is governed by the following equation [16]:

$$c_R \approx \frac{0.87 + 1.12v}{1 + v} \sqrt{\frac{E}{2\rho(1 + v)}}, \qquad (1)$$

where v indicates the Poisson's ratio, E is the Young's modulus, and ρ is the density of the material.

For a multilayer system of different elastic properties, the propagating wave is influenced by the elastic parameters of all the layers that it probes. In the presence of different elastic parameters of all the layers, the Rayleigh wave motion is changed. Thus, the relation between phase velocity and frequency (dispersion curve) contains information about the elastic parameters of the material. For a broadband Rayleigh impulse, it can be considered as a superposition of waves with different frequencies. When traveling in a medium, the higher frequency components that have a lower penetration depth are more influenced by the layer, while the lower components that have a deeper penetration depth are more influenced by the substrate. Thus, the phase velocity of the Rayleigh wave becomes a function of frequency.

China was the first country to produce porcelain. Up to the present time, many kinds of porcelain have been produced in various kiln sites. Most of them were made of clays from local areas, so a difference in element content and their ratios may be expected. Also, the manufacturing processes varied from kiln site to kiln site. Therefore, the elastic properties are different. As a result, the velocities of the Rayleigh waves of the porcelains from different kiln sites are distinct.

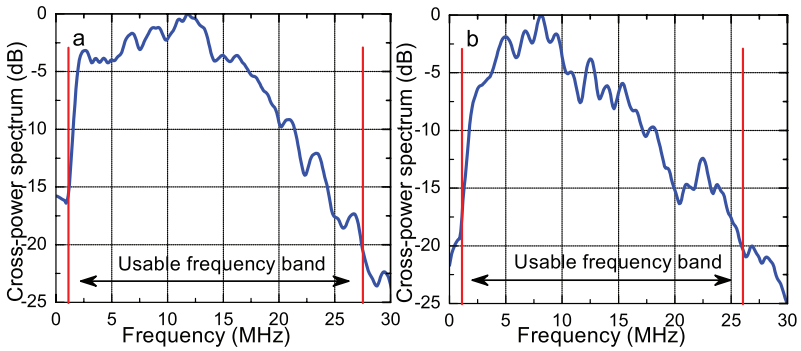

Figure 3. Cross-power spectrum of signals detected at 2 mm and 6 mm of sample (a) A1, (b) B.

Figure 1 shows the experimental arrangement for the laser photoacoustic generation and detection of Rayleigh waves. A Q-switched Nd:YAG laser of 6 ns pulse duration at 1064 nm was used to initiate Rayleigh waves, with 5 Hz repetition rate. Then the laser pulses were directed through an adjustable rectangular aperture which was used to get rid of the stray light. By adjusting the voltage of the power supply of the laser, the pulse energy measured after the rectangular aperture is capable of being regulated within the thermoelastic range. The laser pulses were focused into a thin line by a cylindrical lens and then directed onto the sample surface as a line source. A translation stage was used to modulate the distance between the sample surface and the cylindrical lens.

The broadband Rayleigh waves were monitored by a simple optical fiber interferometer which consists of a 1544 nm continuous wave laser with an output power of 7 mW, a three-port optical fiber circulator and a 1 GHz photodetector. The continuous laser light is coupled into the first port of the circulator by a single model fiber. As it arrives at the tip of the second port, part of the light will be reflected by the optical fiber output face which was carefully cut by a fiber cleaver. The rest of the light normally irradiates on the sample surface and part of the reflected light will be coupled back into the fiber. To achieve favorable sensitivity, the distance between the fiber face and sample surface can be adjusted by setting the fiber tip on a three-dimensional (3D) translation stage. Eventually, the two beams interfere due to their different optical path lengths. The final interference light was detected by the photodetector at the third port and displayed by a 2 GHz digital oscilloscope. The laser pulse was detected by another photodetector before the rectangular aperture and served as a trigger signal. The 3D translation stage, which can move in mutually perpendicular directions with 0.01 mm precision, guarantees that signals of different positions away from the line source can be detected. The distance between the fiber tip and sample surface is 1 mm or below, therefore a slight angular misalignment of fiber has little or no influence on the signals. The wave signals stored by the oscilloscope were transferred to a computer for further analysis. Since the laser source wavelength of the optical fiber interferometer is 1544 nm, our system can be applied to all of those porcelains that can reflect light of this wavelength theoretically.

To decrease the measuring uncertainty and determine the useful bandwidth, two wave signals at different positions were

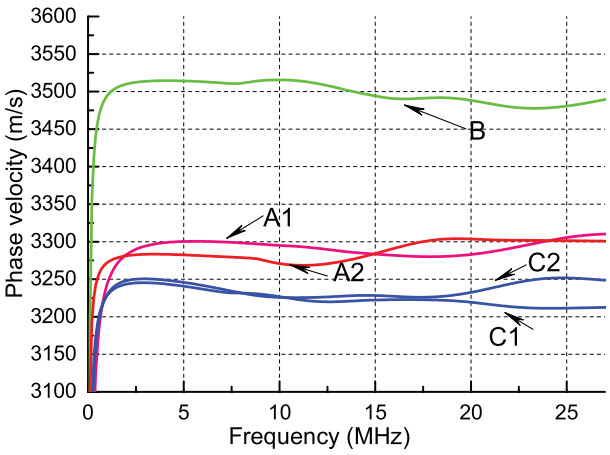

Figure 4. Rayleigh phase velocity versus frequency (dispersion curve) for porcelain of different kiln sites.

cross-correlated and then Fourier transformed. The phase differences of the two signals were calculated by

$$\varphi_1(\omega) - \varphi_2(\omega) = \arctan\left[\frac{\mathrm{Im}(u(\omega))}{\mathrm{Re}(u(\omega))}\right] + 2n\pi \qquad (2)$$

$u(\omega)$ is the cross-power spectrum. The $2n\pi$ uncertainty is determined from the group delay time (the accuracy is 1×10^{-9} s for a sample rate of 10^9 Hz) of the signals [17]. The phase velocity of the harmonic wave with frequency f can be calculated by the following equation:

$$v_p(f) = \left|\frac{(x_2 - x_1)2\pi f}{\varphi_2(f) - \varphi_1(f)}\right|. \qquad (3)$$

The experiments were carried out on five pieces (A1, A2, B1, C1, C2) of porcelain from three different kiln sites (A, B, C). A1 and A2 are from different porcelains while C1 and C2 are the different part of the same porcelain. No special surface preparation, such as polishing, was needed. The length of the line source remains 2 mm. The distance between the lens and porcelain surface was adjusted for practical application. Our experiments were carried out with little or no damage to the samples.

Figure 2 shows the normalized Rayleigh waves detected on various porcelains under the same condition. The first detected point was 2 mm away from the source, and then it moved away on the perpendicular bisector of the line source by 1 mm

Table 1. The average velocity difference between two samples.

Samples	A1–A2	C1–C2	A2–C2	A1–C2	A2–C1	A1–C1	A1–B	A2–B	B–C2	B–C1
Vd (m s^{-1})	4.4	12.4	51.6	60.0	64.0	68.4	206.0	210.4	262.0	274.4

increments. In each group, the waveforms detected at 2 mm and 6 mm were chosen for analysis. So the final results show the average information of the sample at a distance of 4 mm.

Figure 3 shows the cross-power spectrum of signals detected at 2 mm and 6 mm of sample A1 (a), B (b). The useful frequency band is chosen to be 2–26 MHz for −20 dB level. Outside this band, the signal-to-noise ratio decreases drastically, which is of no interest to us.

Figure 4 illustrates the dispersion curves obtained by using the method mentioned above. Since the measurement accuracy of distance and group delay time are 0.01 mm and 1×10^{-9} s respectively, the typical error of velocity is $\Delta V/V \leqslant 1.7 \times 10^{-3}$ with $\Delta V \approx 5.5$ m s^{-1} in our experiment. From figure 4, we can see that the velocity of sample B is the highest while it is the lowest for sample C1. Moreover, the speed disparities between the different part of the same sample (C1, C2) and the different samples from the same kiln sites (A1, A2) are much smaller than the disparities between samples from different kiln sites (such as B and A1). For C1 and C2, the phase velocity lower than 20 MHz shows good agreement with each other, which indicates that our experiment performs with good stability and repeatability. The discrepancies above 20 MHz are most probably due to the differences of the condition of the sample surface and a slight degree of difference in operation, which was inevitable. However, they have no influence in our experiment and should be ignored.

Table 1 tabulates the differences of average velocities between two samples. From this table, it can be seen that the smallest velocity difference between two samples of the different kiln sites is 51.6 m s^{-1}, which is much greater than the largest velocity difference (12.4 m s^{-1}) between two samples of the same kiln sites. The minimum velocity absolution is 12.4 m s^{-1}, below which we cannot distinguish the porcelains of different provenance. Certainly, this method is also suitable to distinguish the porcelains produced by different procedures.

3. Conclusion

In conclusion, we have experimentally demonstrated the evaluation of the Rayleigh phase velocity of porcelains employing the laser photoacoustic system. On the basis of our experiment, we can conclude that the differences of Rayleigh phase velocities of the porcelains from the same kiln site are much smaller than the porcelains from the different kiln sites. Compared to the traditional study methods, the scheme shows some advantages, including noncontact, non-destructivity, simplicity, flexibility and high sensitivity. Furthermore, no particular preparation of the sample surface is needed. All these exciting results make our method a potential application in the provenance study on porcelains. Further studies will make our technique a useful tool for porcelain identification.

Acknowledgments

The authors acknowledge the support from the Hubei Provincial Department of Education (Grant Nos. Q20151903) and Hubei University for Nationalities (Grant Nos. 4148023).

References

[1] Adriaens A 2005 *Spectrochim. Acta* B **60** 1503
[2] Schreiner M, Frühmann B, Jembrih-Simbürger D and Linke R 2004 *Powder Diffr.* **19** 3
[3] Beal J and Olmez I 1997 *J. Radioanal.* **221** 9
[4] Chen T, Rapp G R, Jing Z C and He L 1999 *J. Archaeol.* **26** 1003
[5] Paama L, Pitkänen I and Perämäki P 2000 *Talanta* **51** 349
[6] Bruno P, Caselli M, Curri M L, Genga A, Striccoli R and Traini A 2000 *Anal. Chim. Acta* **410** 193
[7] Li B, Zhao J X, Greig A, Collerson K D, Feng Y X, Sun X M, Guo M S and Zhuo Z X 2006 *J. Archaeol. Sci.* **33** 56
[8] Xiang G, Jiang Z, He M and Hu B 2005 *Spectrochim. Acta* B **60** 1342
[9] Leung P and Luo H 2000 *X-Ray Spectrom.* **29** 34
[10] Wen R, Wang C, Mao Z, Huang Y and Pollard A 2007 *Archaeometry* **49** 101
[11] Pasquini C, Cortez J, Silva L M C and Gonzaga F B 2007 *J. Braz. Chem. Soc.* **18** 463
[12] Fomitchov P A, Kromine A K and Krishnaswamy S 2002 *Appl. Opt.* **41** 4451
[13] Hess P 1996 *Appl. Surf. Sci.* **106** 429
[14] Tu S J, Zhan L, Qian K and Luo S Y 2013 *Laser Phys. Lett.* **10** 025602
[15] Wang H C, Fleming S, Lee Y C, Law S, Swain M and Xue J 2009 *Opt. Express* **17** 15592
[16] Viktorov I A 1967 *Rayleigh and Lamb Waves: Physical Theory and Applications* (New York: Plenum)
[17] Schneider D, Schwarz T and Schultrich B 1992 *Thin Solid Films* **219** 92